Water Research 262 (2024) 122123

Contents lists available at ScienceDirect

Water Research

journal homepage: www.elsevier.com/locate/watres

A novel pretreatment method for analysis the oxygen isotopic compositions of inorganic phosphorus pools in freshwater sediment

Zuxue Jin [a,d], Jingfu Wang [a,b,d,*], Dengjun Wang [c], Shuoru Qiu [a], Jiaojiao Yang [a,b], Wen Guo [a,b], Yiming Ma [a], Xinping Hu [a,b], Jingan Chen [a,b,d,*]

[a] State Key Laboratory of Environmental Geochemistry, Institute of Geochemistry, Chinese Academy of Sciences, Guiyang, 550081, PR China
[b] University of Chinese Academy of Sciences, Beijing, 100049, PR China
[c] School of Fisheries, Aquaculture and Aquatic Sciences, Auburn University, Auburn, AL 36849, USA
[d] Guizhou Province Field Scientific Observation and Research Station of Hongfeng Lake Reservoir Ecosystem, Guiyang, 551499, PR China

ARTICLE INFO

Keywords:
Oxygen isotopic compositions of phosphate ($\delta^{18}O_P$)
Sediment
Phosphorus
Zr-Oxides gels
Pretreatment method

ABSTRACT

Identifying the sources and cycling of phosphorus (P) is particularly important for formulating effective P management strategies in inland water. The oxygen isotopic compositions of phosphate ($\delta^{18}O_P$) are recognized as a promising tool to solve this problem. However, the application of $\delta^{18}O_P$ in freshwater sediment is currently constrained by multiple difficulties. In this study, we presented a novel pretreatment method for $\delta^{18}O_P$ analysis of sediment inorganic P pools. Our results showed that the new method has advantages of simple operation, less time-consuming, and high P recovery rates. Specifically, we replaced the traditional Mg-induced co-precipitation (MAGIC) method by introducing Zr-Oxides gels with high selective adsorption function for phosphate. This made subsequent processing simpler and reduced the time consumption to ~10 days, and the range of P recovery rates were from 88 % to 104 %. Furthermore, we emphasized the necessity of vacuum roasting following lyophilized Ag_3PO_4 to eliminate residual oxygen-containing impurities (e.g., NO_3^-, Ag_2O, and organic matter). Additionally, evidences from microscopy and spectroscopy confirmed that this method ultimately yielded high-purity Ag_3PO_4 with the Ag:P molar ratios of 3.35:1. Importantly, combining direct synthesis Ag_3PO_4 between KH_2PO_4 and $AgNO_3$ with the Ag_3PO_4 obtained by the method revealed no stark oxygen isotopic fractionation of phosphate during the pretreatment processes. The newly established $\delta^{18}O_P$ pretreatment methods here can also be extended to broader studies of the biogeochemical cycling of P in aquatic ecosystems, potentially advancing the understanding of the global P cycle.

1. Introduction

Harmful algal blooms (HABs) have become as one of the most severed environmental problems on the Earth, posing significant economic and ecological threats to both aquatic organisms and public health. The maximum bloom area on the Earth over the past four decades reached 33.27×10^4 km^2, representing 11.7 % of the global lake area (Hou et al., 2022). The most concerned impacts of HABs are the production of toxins in drink-water resources, which can result in illness and/or even mortality of humans and animals (Carmichael, 1994). For instance, acute liver failure was found in 100 out of 131 patients caused by exposure to microcystin (produced by cyanobacteria) in Brazil in 1996, and then 52 out of the 76 deaths could be directly attributed to microcystin (Carmichael et al., 2001). Recently, 330 elephants died in Botswana triggered by drinking microcystin-contaminated waters (https://www.bbc.com/news/world-africa-54234396). Unfortunately, the frequency, magnitude, duration, and severity of HABs appears to be increased in the global freshwater lakes in the coming decades due to intensified global warming and human activities (Paerl and Huisman, 2008; O'Neil et al., 2012; Paerl and Paul, 2012; Hou et al., 2022). Phosphorus (P) is one of the culprits for HABs.

Identifying the sources and cycling of P is first step for the prevent and control of HABs, however, which is challenging. This is mainly because P has a single stable isotope (^{31}P) and numerous radioisotopes with short half-lives (< 26 d), making source identification comparatively difficult (Jaisi and Blake, 2014). Fortunately, P exists mainly as

* Corresponding authors at: State Key Laboratory of Environmental Geochemistry, Institute of Geochemistry, Chinese Academy of Sciences, Guiyang, 550081, PR China.
E-mail addresses: wangjingfu@vip.skleg.cn (J. Wang), chenjingan@vip.skleg.cn (J. Chen).

https://doi.org/10.1016/j.watres.2024.122123
Received 13 May 2024; Received in revised form 24 June 2024; Accepted 20 July 2024
Available online 22 July 2024

orthophosphate (e.g., PO_4^{3-}, HPO_4^{2-}, $H_2PO_4^-$) in nature with a strong bond energy between P and oxygen (359.8 kJ mol^{-1}) and the P-O bonds cannot be breaked under physicochemical processes on the Earth surface (Longinelli and Nuti, 1973; Blake et al., 1997; McLaughlin et al., 2004; Zhao et al., 2021). Furthermore, oxygen has three stable isotopes (^{18}O, ^{17}O, ^{16}O). Therefore, the oxygen isotopic compositions of phosphate ($\delta^{18}O_P$) can be used to trace the P sources and its biogeochemical processes (Elsbury et al., 2009; Joshi et al., 2015; Pistocchi et al., 2017). Since the pioneering work by Tudge. (1960) who developed the analysis method of the oxygen isotopic composition of PO_4 ($\delta^{18}O_P$), and $\delta^{18}O_P$ has been successfully applied to estimate the paleotemperature. Over recent decades, $\delta^{18}O_P$ has been gradually applied to trace the sources and cycle of P on the Earth's surface environment (Colman et al., 2005; Young et al., 2009; Jaisi and Blake, 2010; Tamburini et al., 2012; Gooddy et al., 2015; Joshi et al., 2015, 2016; Granger et al., 2017; Pistocchi et al., 2017; Ishida et al., 2019; Lei et al., 2019; Tian et al., 2020; Wang et al., 2021; Zhao et al., 2021).

Even, the pretreatment of $\delta^{18}O_P$ from environment samples has been a major obstacle for the $\delta^{18}O_P$ analysis. Currently, two kinds of common use methods for the pretreatment of $\delta^{18}O_P$ are concluded as follows: these steps conclude i) PO_4 enrichment by magnesium-induced co-precipitation (MAGIC) (Karl and Tien, 1992); ii) removal of dissolved organic matter (DOM) by applying DAX-8 resin (Zohar et al., 2010; Joshi et al., 2015); iii) formation the precipitations of ammonium phospho-molybdate (APM) and magnesium ammonium phosphate (MAP) or $CePO_4$ precipitation (Tudge, 1960; McLaughlin et al., 2004); iv) removal of Cl^- and HCO_3^- by using KAc-HAc solution and HNO_3, respectively (Zohar et al., 2010; Liu et al., 2019); v) removal of Ce_3^+ and/or other cations by using cation exchange resin (Mclaughlin et al., 2004; Zohar et al., 2010; Joshi et al., 2015); vi) Ag_3PO_4 precipitation (Crowson and showers, 1991); vii) high-purity Ag_3PO_4 solid obtained by recrystallization or adding H_2O_2 to remove residual organic matter (OM) (Joshi et al., 2015; Liu et al., 2019).

However, applying these methods to lacustrine sediment still make it difficult and/or unsuccessful to obtain adequately high-purity Ag_3PO_4. Here, at least two major aspects for the final Ag_3PO_4 solid are reflected on the pretreatment of $\delta^{18}O_P$ in freshwater sediment samples. One of these involves the how to effectively remove the higher contents of OM and metal elements of freshwater sediment relative to other samples (e.g., lake water, marine sediment) (Jaisi and Blake, 2010, 2014; Pistocchi et al., 2017; Yuan et al., 2019; Lei et al., 2020). A second involves the PO_4 recovery rates during the processing. The PO_4 recovery rates might be decreased due to tedious precipitation steps (e.g., Xu et al., 2018; Lei et al., 2020), which potentially resulted in comparable deviations between measured and expected $\delta^{18}O_P$ values. Taken above-mentioned into consideration, it is urgently needed to develop a method with simpler operation of pretreatment, stable PO_4 recovery rates, and high-purity Ag_3PO_4 for analysis the $\delta^{18}O_P$ of different P pools in the freshwater sediment.

Zr-Oxides has been widely used for PO_4 removal, measurement, and enrichment due to its highly efficient selective adsorption for PO_4 (Chitrakar et al., 2006; Ding et al., 2010). Moreover, the adsorbed PO_4 can be easily eluted by NaOH solution. Recently, our group developed a pretreatment method for analysis the $\delta^{18}O_P$ for freshwater water samples, which established on Zr-Oxides gels with selective adsorption function for PO_4 (Liu et al., 2021). However, applying the methods for the $\delta^{18}O_P$ analysis of sediment P pools still faces large challenges. For instance, the Zr-Oxides gels were directly used to adsorb sediment PO_4 extracted by 0.1 M NaOH solution, and even the filtrates' pH was random readjusted to anywhere, all of which are hardly effective. Further, the presence additional O sources including high concentrations of HCO_3^- and Ac^- from extractants, and higher concentrations of dissolved organic carbon (DOC) and SO_4^{2-} within sediment relative to water samples can bias the $\delta^{18}O_P$ signals. Such situations represent a fundamental barrier to apply the $\delta^{18}O_p$ methods of water samples reported by Liu et al. (2021) to the pretreatment of $\delta^{18}O_p$ in freshwater sediment.

Here, we addressed these obstacles and expanded beyond this to develop an effective method for the pretreatment of the $\delta^{18}O_P$ in different P pools of lake sediment, which is currently not available. We solved three fundamental problems regarding pretreatment of $\delta^{18}O_P$: i) how to reduce the pretreatment steps; ii) how to ensure the PO_4 recovery rates during the pretreatment steps; and iii) how to obtain the high-purity Ag_3PO_4.

2. Materials and methods

2.1. Study areas and sample collection

Study areas included Lake Dianchi (102°36′–102°47′ E, 24°40′–25°02′ N), Lake Erhai (100°6′–100°18′ E, 25°36′–25°57′ N), and Hongfeng Reservoir (106°19′–106°28′ E, 26°26′–26°35′ N), all of which are located in the Yunnan-Guizhou Plateau, Southwest China that are facing risks of HABs (Chen et al., 2019; Ji et al., 2022; Jin et al., 2022, 2023a).

In April 2021, sediment samples (Fig. S1) in above-mentioned two lakes and one reservoir were collected by using a Petersen grab sampler (PBS-411, Wuhan Petersen Technology CO., LTD, China). Then, sediment samples were placed into 50 mL clean centrifuge tubes. The temperature of bottom water (above 0.5 m of sediment) was measured by using a multi-parameter water quality monitor (YSI, 6600V2, Co, USA). Porewater samples were obtained by centrifuging (at 4390 g for 15 min) sediment samples. All of samples were stored at 4℃ immediately after collection to minimize microbial activity.

2.2. Sequential extraction

Sediment samples were frozen at −80℃ before freeze drying. Subsequently, these samples were ground and sieved through a 200 mesh and then stored at -20℃ until analysis. Sediment P pools were extracted by using a combined sequential extraction method (Ruttenberg, 1992; Rydin, 2000). These P pools were divided into five pools, including I) loosely sorbed-P, II) Fe-bound P (Fe-P), III) aluminum-oxide bound P (Al-P), IV) authigenic carbonate fluorapatite + biogenic apatite + $CaCO_3$- associated P (Au-P), and V) detrital apatite P (De-P). The steps of sequential extraction before Au-P pool were followed by the report proposed by Rydin (2000), and the following two steps were proposed by Ruttenberg (1992) (details by Fig. S2). Briefly, sediment sample (3.3 g) was placed into a 250 mL centrifuge bottle (Nalgene, USA). Then, 200 mL of extractant (1 M NH_4Cl (pH=7), 0.11 M $NaHCO_3/Na_2S_2O_4$, 0.1 M NaOH, 1 M NaAc (pH=4.0), and 1 M HCl) were used to extract loosely sorbed-P, Fe-P, Al-P, Au-P, and De-P, respectively. All extracts were centrifuged at 4390× g for 15 min and filtered through 0.45 μm filters (TJMF50, Tianjin Jinteng Experimental Equipment CO., LTD, China). The residual sediment was washed by using 200 mL ultrapure water after each of extraction, such operation was repeated three times to reduce P re-adsorption onto residual sediment surface (Liu et al., 2019). Concentrations of inorganic P (P_i) in the filtrates were determined by using the molybdenum blue method (Murphy and Riley, 1962) or ion chromatograph (ICS90, Dionex Co, Ltd, USA).

2.3. The pretreatment of $\delta^{18}O_P$ in sediment P_i pools

We developed a pretreatment method for analysis the $\delta^{18}O_P$ in sediment P_i pools (Fig. 1) based on the methods recommended by McLaughlin et al. (2004), Zohar et al. (2010), and Liu et al. (2019, 2021). Sediment samples from three sites (DC1, HF2, and EH1) were selected as preliminary experiment based on the color of the filtrates extracted by 0.1 M NaOH (Fig. S3). Owing to the low P contents of sediment extracted by NH_4Cl (generally < 5 mg kg^{-1}) (Yang et al., 2022), we were not able to obtain the sufficient contents of Ag_3PO_4 for analysis the $\delta^{18}O_P$ in the P_i pool; so, the pretreatment steps in the P_i pool

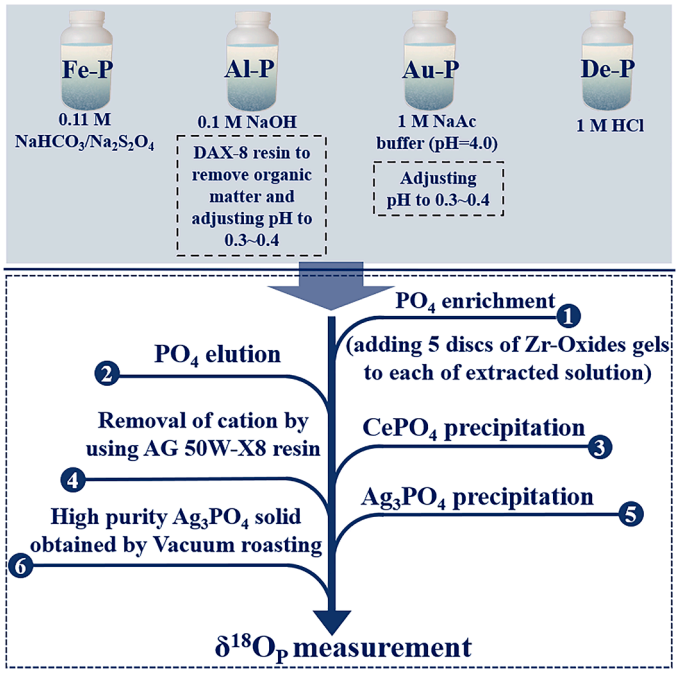

Fig. 1. Purification steps for Ag_3PO_4 of different P_i pools in sediment.

were neglected. The detailed pretreatment steps of $\delta^{18}O_P$ in other P_i pools were established as follows:

i) The $\delta^{18}O_P$ pretreatment of Fe-P and De-P.

Step 1: PO_4 enrichment. Five discs of Zr-Oxide gels (EasySensor Ltd., Nanjing, China; www.easysens or.net) were placed into 250 mL centrifuge bottle with 200 mL filtrates and then shaken for 120 h.
Step 2: PO_4 elution. Zr-Oxide gels loaded with PO_4 were placed into a 50 mL centrifuge tube and eluted with 20 mL 1 M NaOH solution. These tubes were continuously shaken for 24 h or 1 h and the elution steps were repeated 5 or 6 times to ensure the PO_4 recovery rates.
Step 3: $CePO_4$ precipitation. The pH of PO_4 eluate was adjusted to 5.8 using HNO_3 and 2 mL $Ce(NO_3)_3$ solution ($Ce(NO_3)_3{\cdot}6H_2O$, Sigma-Aldrich, USA) (0.5 g $Ce(NO)_3{\cdot}6H_2O$ was dissolved in 2 mL ultrapure water) was added. Then, to turn PO_4 into $CePO_4$ precipitation as much as possible and improve the P recovery rates, 1 M KAc solution was used to re-adjust the pH of the solution to 5.5~5.6 after $CePO_4$ precipitation. After standing for 24 h, the mixture was centrifuged at 4390× g for 15 min and the supernatant was discarded by siphonage to obtain $CePO_4$ precipitation. Noteworthily, the concentrations of Cl^- in the supernatant of all $CePO_4$ precipitations in this study were very low and no macroscopic AgCl precipitation was observed after adding 0.1 M $AgNO_3$ to these supernatants. In contrast, if there are high concentrations of Cl^- in the supernatant of $CePO_4$ precipitation in future samples, the Cl^- will be washed and removed by using buffer solution (pH=5.5) (the pH of solution was adjusted by using 1 M KAc and HAc) (McLaughlin et al., 2004; Liu et al., 2019).
Step 4: Removal cation.

The $CePO_4$ precipitation was dissolved by using approximately 4 mL 1 M HNO_3 and subsequently 16 mL ultrapure water was added into the solution to completely dissolve the precipitation. 10 mL of cation exchange resin (Biorad AG 50W-X8, USA) was added into the mixture and continuously shaken for 12 h to remove cation (e.g., Ce^{3+}). The solution was filtered by using 0.45 μm filters and the cation exchange resin was washed using a small amount of ultrapure water to avoid PO_4 attaching to resin surface.

Step 5: Ag_3PO_4 precipitation and its purification.

The solution was filtrated to a 50 mL black centrifuge tube and its pH was adjusted to 7.3 by using HNO_3 (0.1~1 M), 1 % $NH_3{\cdot}H_2O$, and NaOH solution (5 M). Approximately 15 times of $AgNO_3$ (molar ratio of Ag: P≈15:1) was added into the solution to gradually form Ag_3PO_4 precipitation. Subsequently, to completely turn PO_4 into Ag_3PO_4 precipitation and obtain higher P recovery rates, 1 % $NH_3{\cdot}H_2O$ was used to re-adjust the pH of the solution to 7.3. After standing 24 h, the mixture was centrifuged (4390× g for 15 min) and the supernatant was discarded by siphonage to obtain Ag_3PO_4. The obtained Ag_3PO_4 was washed 1~2 time(s) with ultrapure water to remove the residual impurities (e.g., Ag^+ (with 0.1 M HCl detection), NH_4^+, and NO_3^-). After preprocessing, Ag_3PO_4 samples were frozen-dried at −80℃ for 6 h.

i) The $\delta^{18}O_P$ pretreatment of Al-P.
The filtrate extracted by 0.1 M NaOH contained relatively high contents of natural OM, which needs to be removed by Supelite DAX-8 resin (Sigma Chemical Co) upon shaking for 16 h. Subsequently, the pH of filtrate was adjusted to 0.3~0.4 with HNO_3 after filtration using 0.45 μm filters. The remainder steps were same to i) the $\delta^{18}O_P$ pretreatment of Fe-P and De-P.
ii) The $\delta^{18}O_P$ pretreatment of Au-P.
The $\delta^{18}O_P$ pretreatment steps of Au-P were same as the steps of the $\delta^{18}O_P$ pretreatment of Al-P except the step of removal of OM.

All lyophilized Ag_3PO_4 samples were thoroughly homogenized and placed into quartz tubes. The quartz tubes were pumped to vacuum (1×10^{-2} mbar) and sealed, and then were heated at 450℃ to remove residual oxygen-containing impurities, such as residual OM, NO_3^-, and Ag_2O (Crowson et al., 1991; Blake et al., 2005; Sandy et al., 2013; Jaisi and Blake, 2014; Jin et al., 2023b).

2.4. Characterization of Zr-Oxide gels before and after PO_4 adsorption and Ag_3PO_4

To further investigate the mechanisms of PO_4 adsorption by Zr-Oxide gels, the surface properties of Zr-Oxides gels before and after PO_4 adsorption were characterized by using X-ray photoelectron spectroscopy (XPS), Fourier transform infrared (FTIR), and energy dispersive X-ray spectroscopy (EDS). The mechanisms of PO_4 adsorption by Zr-Oxides gels were available in Supplementary Material. Ag_3PO_4 was also characterized by using scanning electron microscopy (SEM) linked with EDS and X-ray diffraction (XRD) to further identify its purity.

2.5. Analysis the oxygen isotopic composition of PO_4 and water

The analysis of $\delta^{18}O_P$ was referenced in our previous study (Jin et al., 2023b). Triplicate Ag_3PO_4 samples (approximately 0.5 mg) were weighted for each TC/EA run and these samples were stored at oven with the temperature of 60℃ at least for 6 h before its isotopic analysis. The $\delta^{18}O_P$ of these samples was measured by using a Thermo Chemolysis Elemental Analyzer (TC/EA) associated with a gas isotope ratio mass spectrometry (HT- IRMS, Flash EA 1112, Mat 253, Thermo Co, Ltd) in the Third Institute of Oceanography, the Ministry of Natural Resources, China. All $\delta^{18}O_P$ data were calibrated by using two oxygen isotopic reference materials: Ag_3PO_4 (21.7 ± 0.3 ‰, B2207, Elemental Microanalysis, UK) and Benzoic acid (IAEA-601, 23.3 ± 0.3 ‰). $\delta^{18}O_P$ values had an analytical precision better than ±0.3 ‰ based on repeated measurements of Ag_3PO_4 standard samples. All values of $\delta^{18}O_P$ are reported relative to the Vienna Standard Mean Ocean Water (VSMOW), calculated as:

$$\delta^{18}O(‰) = \left[\frac{R(^{18}O/^{16}O_{sample})}{R(^{18}O/^{16}O_{VAMOW})} - 1\right] \times 1000 \quad (1)$$

Note: R ($^{18}O/^{16}O$) represents the oxygen isotopic abundance ratio.

The oxygen isotopic values of porewater were analyzed by using an LGR Isotopic Water Analyzer.

3. Results and discussion

3.1. PO_4 recovery rates of key steps of sample pretreatment

Identifying Zr-Oxides gels with the adsorption capacity for PO_4 extracted by sequential extraction was the first step for PO_4 enrichment due to the interference of various impurities (e.g., anion, cation, and DOM). The PO_4 adsorption capacity (~2270 μg P/five discs of Zr-Oxides gels) was reported by in a simulated freshwater water bodies in our recent study (Liu et al., 2021). To further elucidate the characteristics of PO_4 adsorption by Zr-Oxides gels in different extracts, we selected sediment samples from three sites (DC1, HF2, and EH1) based on the color of the filtrates (Fig. S3) extracted by 0.1 M NaOH to perform continuous observations at the beginning of experiment. Here, to improve the PO_4 recovery rates, PO_4 of the filters was required to continually adsorb by Zr-Oxides gels as much as possible. Therefore, we did not stop the adsorption experiment until 120 h. Similarly, Zr-Oxides gels loaded with PO_4 were eluted by using 1 M NaOH solution each of 24 h and the step was repeated 5 times to avoid the fractionation of the $\delta^{18}O_P$ due to incomplete elution. The PO_4 recovery rates after PO_4 elution for 120 h ranged from 88.3 % to 108.1 % (not shown). Based on above-mentioned results, we further performed PO_4 enrichment by Zr-Oxides gels from all filtrates in all sample sites (Fig. S1). Results suggested that the range of PO_4 recovery rates in the PO_4 enrichment, $CePO_4$, and Ag_3PO_4 precipitation steps from different sediment P_i pools are from 89.5 ± 5.6 % to 105.0 ± 6.6 %, from 99.7 ± 0.2 % to 99.9 ± 0.1 %, and from 98.8 ± 0.7 % to 99.3 ± 0.4 %, respectively (Table 1). And then the total PO_4 recovery rates varied from 88.2 ± 5.2 % to 104.2 ± 6.9 % (Table 1). Alternatively, at the step of PO_4 elution (see section 2.3), the Zr-Oxides gels of adsorbed PO_4 were also continually shaken for 1 h and the elution steps were repeated 6 times to ensure the PO_4 recovery rates (Fig. S4a–d). The PO_4 recovery rates after PO_4 elution ranged from 81.4 ± 0.4 % to 96.1 ± 0.3 % (Table S1), the total PO_4 recovery rates at the pretreatment steps of $\delta^{18}O_P$ varied from 80.7 % to 94.8 % according to the PO_4 recovery rates between $CePO_4$ and Ag_3PO_4 precipitation (Tables 1 and S1), demonstrating this method with high PO_4 recovery rates.

3.2. Removal of impurities in PO_4 enrichment and its elution

We next evaluated the removal rates of impurities in PO_4 enrichment and its elution steps, the measured methods for these impurities were available in Supplementary Material. In contrast to the $\delta^{18}O_P$ methods of water bodies reported by Liu et al. (2021), the removal efficiencies of DOC in the extracts from Al-P pools (extracted by 0.1 M NaOH) were not such high-efficiency. The former was higher than 99 % in the simulated freshwater water bodies removed by using Zr-Oxides gels, whereas the latter was less than 50 % removed by DAX-8 resin (Table S2). Compared to DOC contents of De-P pools (10.6 ± 2.8 mg), the DOC contents in the Fe-P pool (69.2 ± 2.4 mg) and Au-P pools (14102.6 ± 615.7 mg) were substantially higher, which was likely attributed to their corresponding extractants (e.g., $NaHCO_3$, NaAc, and HAc) (Table S2). The removal efficiencies of DOC in the extracted solution of Fe-P and Au-P were less than 72 % and higher than 97 %, respectively (Table S2). Cl^- and SO_4^{2-} were the main two kinds of anions in all the extracts (Table S2). The highest contents of Cl^- (~16,268.7 mg) and SO_4^{2-} (9808.5 mg) were observed in the extracts of De-P pool and the extracts of Fe-P pool, respectively, which was primarily attributed to the extractants (e.g., HCl and $Na_2S_2O_4$). Fortunately, higher than 99 % of Cl^- and SO_4^{2-} could be removed by the steps of PO_4 enrichment and its elution in these P pools (Table S2). The removal efficiencies of metal elements (e.g., Mg, Cr, Mn, Fe, Cu, Zn, As, Sb, Ba, and Pb) of the extracts after PO_4 enrichment and elution were shown in Table S3. The removal rates of these elements were higher than 91.0 % besides As in the extracts of all P pools at three sample sites, Cr in the extracts of all Fe-P pool at three sample sites, and Cu in the Fe-P pool at sample sites DC1 and EH1 (Table S3).

The residual impurities, encompassing metal elements and oxygen-containing impurities (e.g., DOM, NO_3^-, Ag_2O, and intracrystalline water), were further removed by the cation exchange resin and vacuum roasting of Ag_3PO_4, respectively (Fig. 1). Besides external oxygen-containing impurities (e.g., DOM, NO_3^-, water), we noted that it is inevitable to generate Ag_2O during the formation Ag_3PO_4 precipitation and thereby causes the deviation relative to the expected $\delta^{18}O_p$ values (Mine et al., 2017; Xu et al., 2018). Vacuum roasting of Ag_3PO_4 is usually considered as the final purification step before the analysis of $\delta^{18}O_p$ (Crowson et al., 1991; Blake et al., 2005; Sandy et al., 2013; Jaisi and Blake, 2014; Mine et al., 2017; Jin et al., 2023b). All these oxygen-containing impurities in the Ag_3PO_4 can be removed by using the method (Crowson et al, 1991; Blake et al., 2005; Sandy et al., 2013; Jaisi and Blake, 2014).

3.3. The purity of Ag_3PO_4

Ag:P molar ratios of Ag_3PO_4 have been gradually used to estimate the purity of the Ag_3PO_4 solid (Mine et al., 2017). SEM and EDS results demonstrated that the Ag:P molar ratios of Ag_3PO_4 were (3.35 ± 0.12):1 (Fig. 2a–e), similar results were observed by a previous study with the similar Ag:P molar ratios (3.3:1) (Mine et al., 2017). These results of the Ag:P molar ratios were slightly higher than the theoretical Ag:P molar ratio (3:1) of Ag_3PO_4, which indicated the presence of Ag except Ag_3PO_4 in the obtained Ag_3PO_4 solid. The view was further supported by XRD results, suggesting the occurrence of Ag_3PO_4 and Ag in the obtained Ag_3PO_4 solid (Fig. 2f). Here, it is worth considering that higher Ag:P molar ratios of the obtained Ag_3PO_4 solid are majorly controlled by two linked but not overlapping variables: $AgNO_3$ and Ag_2O. The former is artificially introduced for crucial steps of Ag_3PO_4 precipitation, whereas the latter is by-product associated with the Ag_3PO_4 precipitation. We consider the fundamental reason that the presence of Ag could be caused by the Ag_2O through vacuum roasting. However, such situation has no effect on the measurement of $\delta^{18}O_p$ compositions in Ag_3PO_4 due to no oxygen occurrence from Ag. Furthermore, Ag_3PO_4 solid is commonly weighed into a small silver cup before the $\delta^{18}O_p$ analysis (Blake et al., 2005; Sandy et al., 2013). Importantly, these Ag:P molar ratios of the obtained Ag_3PO_4 solid are close to 3:1, indicating that the obtained Ag_3PO_4 by our method is high-purity.

3.4. Oxygen isotopic fractionation validation

To further identify whether occurred oxygen isotopic fractionation of PO_4 during the pretreatment processes, therefore, Ag_3PO_4 was generated by using two methods: (1) direct reaction between KH_2PO_4 and

Table 1
PO_4 recovery rates of key steps ($n = 24$).

PO_4 recovery rates of key steps (%)				
P_i pools	after PO_4 elution	$CePO_4$	Ag_3PO_4	Total recovery rates
Fe-P	99.7 ± 6.7	99.9 ± 0.1	99.2 ± 0.2	98.9 ± 6.6
Al-P	95.0 ± 3.1	99.8 ± 0.2	98.8 ± 0.7	93.7 ± 2.9
Au-P	89.5 ± 5.6	99.7 ± 0.2	98.9 ± 0.5	88.2 ± 5.2
De-P	105.0 ± 6.6	99.9 ± 0.1	99.3 ± 0.4	104.2 ± 6.9

Note: PO_4 recovery rates were calculated based on the mass conservation law. After formation $CePO_4$ and Ag_3PO_4 precipitation, the precipitation was centrifuged at 4390 g for 15 min, the supernatant was filtered by using 0.45 μm filters, P concentrations of filtered filtrate were measured by using molybdenum blue method (Murphy and Riley, 1962) and ion chromatograph (ICS90, Dionex Co, Ltd, USA). The PO_4 recovery rates were expressed as mean (μg) ± standard deviation ($n = 24$).

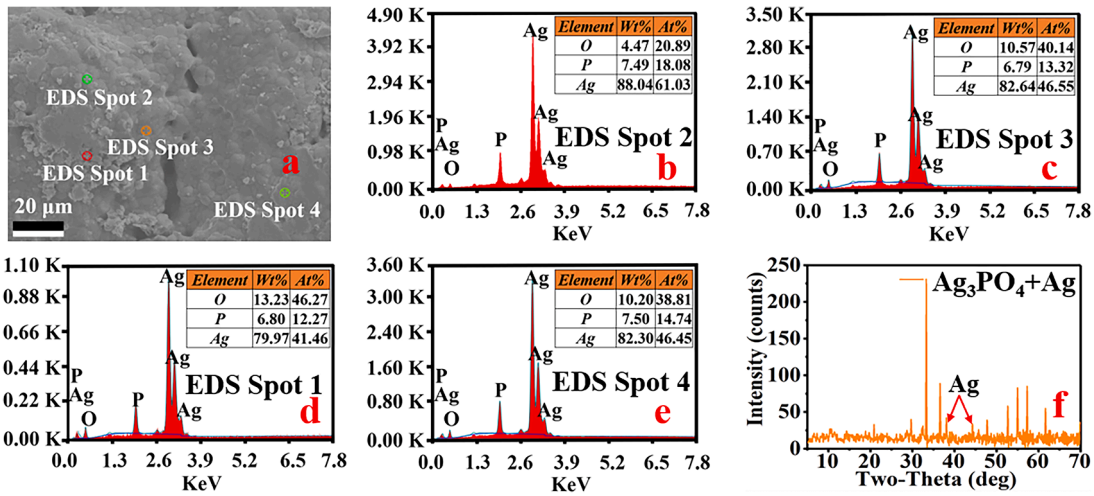

Fig. 2. SEM image, EDS spectrum, and XRD spectrum of Ag_3PO_4. Panel a represents SEM image of Ag_3PO_4. Panel b-e represent the corresponding EDS elements of panel a. Panel f represents XRD patterns of Ag_3PO_4.

$AgNO_3$; (2) following our pretreatment methods (see section 2.3). The values of $\delta^{18}O_p$ in Ag_3PO_4 obtained by using above two methods were 11.5 ± 0.4 ‰ ($n = 5$) and 11.5 ± 0.3 ‰ ($n = 10$) (Fig. S5a), respectively, suggesting that no stark oxygen isotopic fractionations of PO_4 were observed during the pretreatment steps due to their same P sources. In accordance with our recent findings, a study conducted in the lab also found that the $\delta^{18}O_p$ values of obtained Ag_3PO_4 by chemical reaction between KH_2PO_4 and $AgNO_3$ were 11.2 ± 0.3 ‰ (Liu et al., 2019). Further, similar results were also observed in our previous experiments, demonstrating that no pronounced oxygen isotopic fractionations of PO_4 were found in three different P concentrations with the same P sources by using the same method in the simulated freshwater water bodies (Fig. S5b) (Liu et al., 2021). Furthermore, the method was further extended in field and compared with traditional method proposed by McLaughlin et al. (2004), these results also revealed that no obvious oxygen isotopic fractionations of PO_4 were observed in P sources from wastewater, rain seepage, and spring water (Fig. S5c) (Liu et al., 2021).

3.5. The oxygen isotopic compositions of PO_4

To closely assess this stability of the measured instrument during the analysis periods and thus to gain reliable $\delta^{18}O_p$ data, we analyzed the $\delta^{18}O_p$ values of the standard samples of Ag_3PO_4 across the entire measurements. These results (21.7 ± 0.2 ‰ ($n = 35$, panel a) and 21.5 ± 0.2 ‰ ($n = 12$, panel b)) (Fig. 3) indicated that the analytical precision is up to ±0.2 ‰, which reflected that the analytical $\delta^{18}O_p$ data is trustworthy.

The values of $\delta^{18}O_p$ in sediment P_i pools (e.g., Fe-P, Al-P, Au-P, and De-P) varied from 8.1 ‰ to 20.6 ‰ (Fig. 4), similar $\delta^{18}O_p$ ranges (9.8 ‰ ~23.4 ‰) of sediment P_i pools from Lake Tai were also observed (Yuan et al., 2019). Importantly, the $\delta^{18}O_P$ values of different P_i pools in sediments at the different sites in the same lake or reservoir were obviously differentiated (Fig. 4) and most of them were not fallen into the ranges of the oxygen isotopic equilibrium of PO_4 ($\delta^{18}O_{P\text{-}eq}$) calculated by the data from Table S4 and the empirical equation proposed by Chang and Blake (2015) (see Supplementary Material), which possibly inherit the original oxygen isotopic signals of the sole and/or mixed P source(s) and thus can reflect potential P source(s) for these P_i pools (e.g., Joshi et al., 2015). In contrast, if the $\delta^{18}O_P$ values were fallen into the range of $\delta^{18}O_{P\text{-}eq}$, which would reflect the microbial cycling of PO_4, because oxygen isotopic signals of PO_4 can be shifted towards $\delta^{18}O_{P\text{-}eq}$ driven by microorganisms (Jaisi et al., 2011; Stout et al., 2014; Granger et al., 2017). Taken together, the $\delta^{18}O_p$ signals can be used to identify the sources and cycling of P. However, we lack information regarding the $\delta^{18}O_P$ data of potential P sources, the P recycling rates, and the real residence time of sediments in these lakes and reservoir. Therefore, more direct evidences of above-mentioned information are needed to identify the P sources and its biogeochemical cycling of these sediment P_i pools.

There are, however, potential limitations to allow application of the new method between sample types and geographical regions. For instance, the new established pretreatment method of $\delta^{18}O_p$ were based

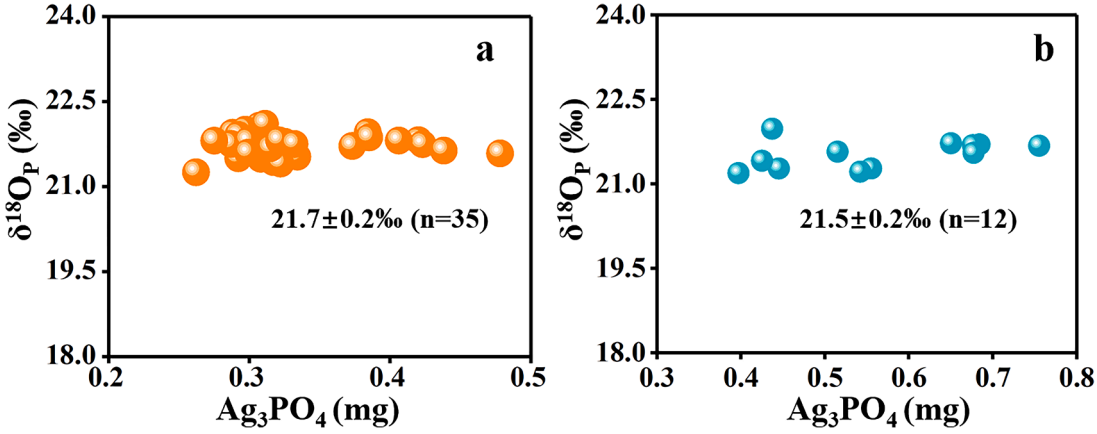

Fig. 3. The oxygen isotopic compositions of Ag_3PO_4. Ag_3PO_4 of panel a was provided by the Third Institute of Oceanography of the State Oceanic Administration of China. Ag_3PO_4 of panel b was provided by us. Two standard samples of Ag_3PO_4 were same ($\delta^{18}O_P$ = 21.7 ‰, B2207, Elemental Microanalysis, UK).

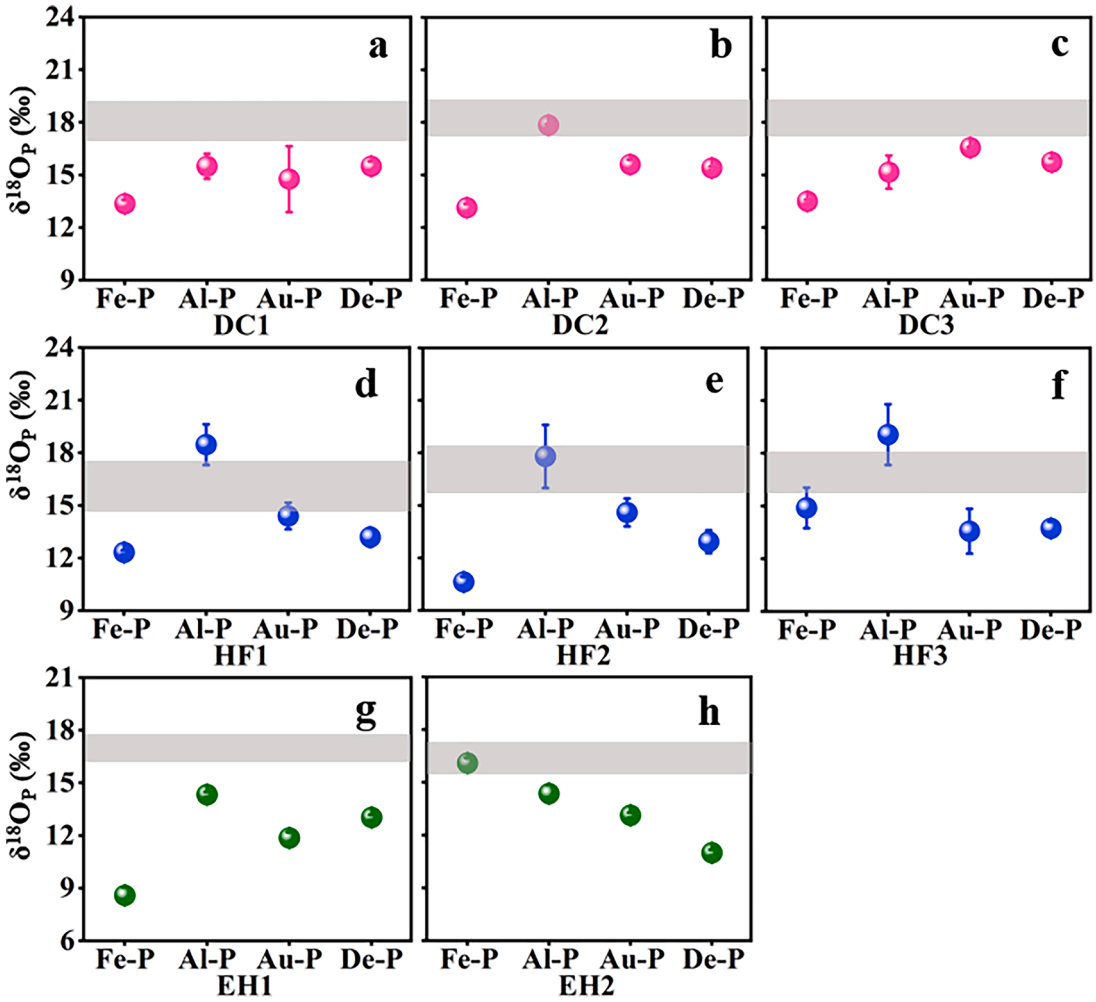

Fig. 4. The values in $\delta^{18}O_P$ of sediment P_i pools. Note: The gray areas represent the expected equilibrium range of $\delta^{18}O_P$ in these lakes and reservoir, the equilibrium was calculated by using the temperature equilibrium formula (Chang and Blake, 2015). Panel a-c, d-f, and g-h represent the $\delta^{18}O_P$ of different P_i pools from Lake Dianchi sediments, Hongfeng reservoir sediments, and Lake Erhai sediments, respectively. The $\delta^{18}O$ of sediment porewater and the range of temperature at sediment-water interface were shown in Table S4. Error bar represents standard deviations of triplicated measurements. Where error bars are not visible, they are smaller than the data symbols.

on the sediments from two lakes and one reservoir, which may not be representative of full breadth of lake and/or reservoir sediments. We encourage future studies to include other environmental samples with the diversity of impurities such as DOM and metal, so that the new method for any types of samples could be applied across different environments.

3.6. Advantages for the pretreatment method relative to previous studies

The advantages for the pretreatment methods of $\delta^{18}O_P$ in this study than previous studies were summarized in Table S5. The main advantages are as follows: i) The multiple precipitation methods for PO_4 enrichment (e.g., Jaisi and Blake, 2010; Nisbeth et al., 2022) were replaced by Zr-Oxides gels with selective adsorption for PO_4; ii) Removal DOM among all of P_i pools in previous studies (e.g., Joshi et al., 2015), but only the P pools extracted by NaOH in this study, were needed; iii) The step of removal Cl^- in previous studies was essential for obtaining high-purity Ag_3PO_4 (e.g., Zohar et al., 2010; Liu et al., 2019), in contrast, the Cl^- concentrations in the supernatant of $CePO_4$ in this study were very low with no formation macroscopic precipitation of AgCl after added $AgNO_3$ solution and thus given up the step; iv) In comparison to the presence of potential oxygen-containing impurities (e.g., NO_3^-) (e.g., Jaisi and Blake, 2014) of Ag_3PO_4 obtained by previous methods without vacuum roasting, the purity of obtained Ag_3PO_4 in this study was higher; v) The obtained Ag_3PO_4 were further required to determine the C and/or N contents before the analysis the $\delta^{18}O_P$ for ensuring the reliable $\delta^{18}O_P$ data in previous studies (e.g., Yuan et al., 2019), but the step in this study was not needed; vi) The pretreatment time in previous studies was approximately 14 days and even longer, which was reduced to 10 days in this study. Taken together, these above-listed advantages led to simpler operation, lesser time-consuming, and high-purity Ag_3PO_4 for the pretreatment of samples. Such advantages of the new method hold a promising potential to significantly advance the study of biogeochemical and dynamic P cycling in various environments.

4. Conclusions

To date, the measurement of $\delta^{18}O_P$ generally transforms PO_4 into Ag_3PO_4. However, the diversity of impurities of freshwater sediment makes it challenging to obtain high-purity Ag_3PO_4 samples, consequently limiting its wide application. Our research offers an innovative approach for the $\delta^{18}O_p$ analysis within different P_i pools of lake sediment, with the benefits of simple operation and less time consumption. Critically, complementary EDS and XRD results suggested that the Ag_3PO_4 obtained through this new method was high-purity.

Importantly, no notable oxygen isotopic fractionations were discerned by comparing the $\delta^{18}O_p$ values of Ag_3PO_4 from the new established method and direct synthesis between KH_2PO_4 and $AgNO_3$. In addition, the standard deviation of oxygen isotopic compositions from Ag_3PO_4 standard samples was better than 0.3 ‰ across the measured processes. These results suggested that our method can yield precise and accurate $\delta^{18}Op$ data from different P_i pools in sediment.

CRediT authorship contribution statement

Zuxue Jin: Writing – original draft, Visualization, Methodology, Investigation, Formal analysis, Data curation. **Jingfu Wang:** Writing – review & editing, Project administration, Methodology, Conceptualization. **Dengjun Wang:** Writing – review & editing. **Shuoru Qiu:** Formal analysis. **Jiaojiao Yang:** Investigation. **Wen Guo:** Formal analysis. **Yiming Ma:** Investigation. **Xinping Hu:** Formal analysis. **Jingan Chen:** Writing – review & editing, Validation, Project administration, Methodology.

Declaration of competing interest

The authors declare that they have no known competing financial interests or personal relationships that could have appeared to influence the work reported in this paper.

Data availability

No data was used for the research described in the article.

Acknowledgements

This study was sponsored jointly by the National Key R&D Plan of China (no. 2021YFC3201000 and 2023YFF0806000), the Strategic Priority Research Program of CAS (no. XDB40020400), the Chinese NSF Project (no. 41977296, 42277253), the Guizhou Provincial Science and Technology Program (Qiankehe Platform Talents-YQK [2023]034, Qiankehe Platform-YWZ[2023]006), the Science and Technology Project of Guizhou Province (Qiankehe Support [2022] general 201), and the Outstanding member of Youth Innovation Promotion Association CAS(Y2023105).

Supplementary materials

Supplementary material associated with this article can be found, in the online version, at doi:10.1016/j.watres.2024.122123.

References

Blake, R.E., O'Neil, J.R., Garcia, G.A, 1997. Oxygen isotope systematics of biologically mediated reactions of phosphate: I. Microbial degradation of organophosphorus compounds. Geochem. Cosmochim. Ac. 61, 4411–4422.
Blake, R.E., O'Neil, J.R., Surkov, A.V., 2005. Biogeochemical cycling of phosphorus: insights from oxygen isotope effects of phosphoenzymes. Am. J. Sci. 305, 596–620.
Carmichael, W.W., 1994. The toxins of cyanobacteria. Sci. Am. 270, 78–86.
Carmichael, W.W., Azevedo, S.M.F.O., An, JS., Molica, R.J.R., Jochimsen, E.M., Lau, S., Rinehart, K.L., Shaw, G.R., Eaglesham, G.K., 2001. Human fatalities from cyanobacteria: chemical and biological evidence for cyanotoxins. Environ. Health Persp. 109, 663–668.
Chang, S.J., Blake, R.E., 2015. Precise calibration of equilibrium oxygen isotope fractionations between dissolved phosphate and water from 3 to 37 °C. Geochim. Cosmochim. Ac. 150, 314–329.
Chen, J.A., Zeng, Y., Yu, J., Wang, J.F., Yang, H.Q., Lu, Y.T., 2019. Preferential regeneration of P relative to C in a freshwater lake. Chemosphere 222, 15–21.
Chitrakar, R., Tezuka, S., Sonoda, A., Sakane, K., Ooi, K., Hirotsu, T., 2006. Selective adsorption of phosphate from seawater and wastewater by amorphous zirconium hydroxide. J. Colloid. Interf. Sci. 297, 426–433.
Colman, A.S., Blake, R.E., Karl, D.M., Fogel, M.L., Turekian, K.K., 2005. Marine phosphate oxygen isotopes and organic matter remineralization in the oceans. Proc. Natl. Acad. Sci. U.S.A. 102 (37), 13023–13028.
Crowson, R.A., Showers, W.J., Wright, E.K., Hoering, T.C., 1991. Preparation of phosphate samples for oxygen isotope analysis. Anal. Chem. 63, 2397–2400.
Ding, S.M., Xu, D., Sun, Q., Yin, H.B., Zhang, C.S., 2010. Measurement of dissolved reactive phosphorus using the diffusive gradients in thin films technique with a high-capacity binding phase. Environ. Sci. Technol. 44, 8169–8174.
Elsbury, K.E., Paytan, A., Ostrom, N.E., Kendall, C., Young, M.B., Mclaughlin, K., Rollog, M.E., Watson, S., 2009. Using oxygen isotopes of phosphate to trace phosphorus sources and cycling of Lake Erie. Environ. Sci. Technol. 43, 3108–3114.
Gooddy, D.C., Lapworth, D.J., Ascott, M.J., Bennett, S.A., Heaton, T.H.E., Surridge, B.W. J., 2015. Isotopic fingerprint for phosphorus in drinking water supplies. Environ. Sci. Technol. 45, 9020–9028.
Granger, S.J., Heaton, T.H.E., Pfahler, V., Blackwell, M.S.A., Yuan, H.M., Collins, A.L., Gan, J., 2017. The oxygen isotopic composition of phosphate in river water and its potential sources in the upper river Taw catchment. UK. Sci. Total Environ. 574, 680–690.
Hou, X.J., Feng, L., Dai, Y.H., Hu, C.M., Gibson, L., Tang, J., Lee, Z.P., Wang, Y., Cai, X.B., Liu, J.G., Zheng, Y., Zheng, C.M., 2022. Global mapping reveals increase in lacustrine algal blooms over the past decade. Nat. Geosci. 15, 130–134.
Ishida, T., Uehara, Y., Iwata, T., Cid-Andres, A.P., Asano, S., Ikeya, T., Osaka, K., Ide, J., Privaldos, O.L.A., De Jesus, I.B.B., Peralta, E.M., Triño, E.M.C., Ko, C., Paytan, A., Tayasu, I., Okuda, N., 2019. Identification of phosphorus sources in a watershed using a phosphate oxygen isoscape approach. Environ. Sci. Technol. 53, 4707–4716.
Jaisi, D.P., Blake, R.E., 2014. Advances in using oxygen isotope ratios of phosphate to understand phosphorus cycling in the environment. Adv. Agron. 125, 1–54.
Jaisi, D.P., Blake, R.E., 2010. Tracing sources and cycling of phosphorus in Peru margin sediments using oxygen isotopes in authigenic and detrital phosphates. Geochim. Cosmochim. Ac. 74, 3199–3212.
Jaisi, D.P., Kukkadapu, R.K., Stout, L.M., Varga, T., Blake, R.E., 2011. Biotic and abiotic pathways of phosphorus cycling in minerals and sediments: Insights from oxygen isotope ratios in phosphate. Environ. Sci. Technol. 45, 6254–6261.
Ji, N.N., Liu, Y., Wang, S.R., Wu, Z.H., Li, H., 2022. Buffering effect of suspended particulate matter on phosphorus cycling during transport from rivers to lakes. Water Res. 216, 118350.
Jin, Z.X., Liao, P., Jaisi, D.P., Wang, D.J., Wang, J.F., Wang, H., Jiang, S.H., Yang, J.J., Qiu, S.R., Chen, J.A., 2023a. Suspended phosphorus sustains algal blooms in a dissolved phosphorus-depleted lake. Water Res. 241, 120134.
Jin, Z.X., Wang, J.F., Jiang, S.H., Yang, J.J., Qiu, S.R., Chen, J.A., 2022. Fuel from within: can suspended phosphorus maintain algal blooms in Lake Dianchi. Environ. Pollut. 311, 119964.
Jin, Z.X., Wang, J.F., Zhang, R.X., Liao, P., Liu, Y., Yang, J.J., Chen, J.A., 2023b. Identification of the sources of different phosphorus fractions in lake sediments by oxygen isotopic composition of phosphate. Appl. Geochem. 151, 105627.
Joshi, S.R., Kukkadapu, R.K., Burdige, D.J., Bowden, M.E., Sparks, D.L., Jaisi, D.P., 2015. Organic matter remineralization predominates phosphorus cycling in the mid-bay sediments in the Chesapeake Bay. Environ. Sci. Technol. 49, 5887–5896.
Joshi, S.R., Li, X.N., Jaisi, D.P., 2016. Transformation of phosphorus pools in an agricultural soil: an application of oxygen-18 labeling in phosphate. Soil Sci. Soc. Am. J. 80, 69–78.
Karl, D.M., Tien, G., 1992. MAGIC: A sensitive and precise method for measuring dissolved phosphorus in aquatic environments. Limnol. Oceanogr. 37 (1), 105–116.
Lei, X.T., Zhang, H., Chen, M., Guo, L.D., Zhang, X.G., Jiang, Z.H., Blake, R.E., Chen, Z. G., 2020. The efficiency of sequential extraction of phosphorus in soil and sediment: insights from the oxygen isotope ratio of phosphate. J. Soil Sediment. 20, 1332–1343.
Lei, X.T., Chen, M., Guo, L.D., Zhang, X.G., Jiang, Z.H., Chen, Z.G., 2019. Diurnal variations in the content and oxygen isotope composition of phosphate pools in a subtropical agriculture soil. Geoderma 337, 863–870.
Liu, Y., Wang, J.F., Chen, J.A., Jin, Z.X., Ding, S.M., Yang, X.H., 2021. Method for phosphate oxygen isotopes analysis in water based on *in situ* enrichment, elution, and purification. J. Environ Manage. 279, 111618.
Liu, Y., Wang, J.F., Chen, J.A., Zhang, R.Y., Ji, Y.X., Jin, Z.X., 2019. Pretreatment method for the analysis of phosphate oxygen isotope ($\delta^{18}O_P$) of different phosphorus fractions in freshwater sediments. Sci. Total. Environ. 685, 229–238.
Longinelli, A., Nuti, S., 1973. Revised phosphate-water isotopic temperature scale. Earth Planet Sci. Lett. 19, 373–376.
McLaughlin, K., Silva, S., Kendall, C., Stuart-Williams, H., Paytan, A., 2004. A precise method for the analysis of $\delta^{18}O$ of dissolved inorganic phosphate in seawater. Limnol. Oceanogr.: Method. 2, 202–212.
Mine, A.H., Waldeck, A., Olack, G., Hoerner, M.E., Alex, S., Colman, A.S., 2017. Microprecipitation and $\delta^{18}O$ analysis of phosphate for paleoclimate and biogeochemistry research. Chem. Geol. 460, 1–14.
Murphy, J., Riley, J.P., 1962. A modified single solution method for the determination of phosphate in natural waters. Anal. Chim. Acta. 26, 31–36.
Nisbeth, C.S., Tamburini, F., Kidmose, J., Jessen, S., O'Connell, D.W., 2022. Analysis of oxygen isotopes of inorganic phosphate ($\delta^{18}O_P$) in freshwater: A detailed method description for obtaining oxygen isotopes of inorganic phosphate in environmental water samples. MethodsX. 9, 101706.
Paerl, H.W., Huisman, J., 2008. Blooms like it hot. Science 320, 57–58.
Paerl, H.W., Paul, V.J., 2012. Climate change: Links to global expansion of harmful cyanobacteria. Water Res. 46, 1349–1363.
O'Neil, J.M., Davis, T.W., Burford, M.A., Gobler, C.J., 2012. The rise of harmful cyanobacteria blooms: the potential roles of eutrophication and climate change. Water Res. 14, 313–334.
Pistocchi, C., Tamburini, F., Gruau, G., Ferhi, A., Trevisan, D., Dorioz, J-M., 2017. Tracing the sources and cycling of phosphorus in river sediments using oxygen

isotopes: methodological adaptations and first results from a case study in France. Water Res. 111, 346–356.
Ruttenberg, K.C., 1992. Development of a sequential extraction method for different forms of phosphorus in marine sediments. Limnol. Oceanogr. 37 (7), 1460–1482.
Rydin, E., 2000. Potentially mobile phosphorus in Lake Erken sediment. Water Res. 34 (7), 2307. -2042.
Sandy, E.H., Blake, R.E., Chang, S.J., Yao, J., Yu, C., 2013. Oxygen isotope signature of UV degradation of glyphosphate and phosphonoacetate: tracing sources and cycling of phosphonates. J. Hazard Mater. 260, 947–954.
Stout, L.M., Joshi, S.R., Kana, T.M., Jaisi, D.P., 2014. Microbial activities and phosphorus cycling: an application of oxygen isotope ratios in phosphate. Geochim. Cosmochim. Ac. 138, 101–116.
Tamburini, F., Pfahler, V., Bünemann, E.K., Guelland, K., Bernasconi, S.M., Frossard, E., 2012. Oxygen isotopes unravel the role of microorganisms in phosphate cycling in soils. Environ. Sci. Technol. 46, 5956–5962.
Tian, L.Y., Guo, Q.J., Yu, G.R., Zhu, Y.G., Lang, Y.C., Wei, R.F., Hu, J., Yang, X.R., Ge, T. D., 2020. Phosphorus fractions and oxygen isotope composition of inorganic phosphate in typical agricultural soils. Chemosphere 239, 124622.
Tudge, A.P., 1960. A method of analysis of oxygen isotopes in orthophosphate-its use in the measurement of paleotemperatures. Geochim. Cosmochim. Ac. 18, 81–93.
Wang, J., Huang, T., Wu, Q.Q., Bu, C.C., Yin, X.J., 2021. Sources and cycling of phosphorus in the sediment of rivers along a eutrophic lake in China indicated by phosphate oxygen isotopes. ACS Earth Space Chem. 5, 88–94.
Xu, Z.F., Huang, T., Yin, X.J., 2018. Improvements in the preparation of phosphate for oxygen isotope analysis from soils and sediments. PLoS ONE 13 (9), e0204203.
Yang, C.C., Li, J.Y., Yin, H.B., 2022. Phosphorus internal loading and sediment diagenesis in a large eutrophic lake (Lake Chaohu, China). Environ. Pollut. 292, 118471.
Young, M.B., McLaughlin, K., Kendall, C., Stringfellow, W., Rollog, M., Elsbury, K., Donald, E., Paytan, A., 2009. Characterizing the oxygen isotopic composition of phosphate sources to aquatic ecosystems. Environ. Sci. Technol. 43 (14), 5190–5196.
Yuan, H.Z., Li, Q., Kukkadapu, R.K., Liu, E.F., Yu, J.H., Fang, H., Li, H., Jaisi, D.P., 2019. Identifying sources and cycling of phosphorus in the sediment of a shallow freshwater lake in China using phosphate oxygen isotopes. Sci. Total. Environ. 676, 823–833.
Zhao, M.Y., Blake, R.E., Liang, Y.H., Ruf, D.D., Jaisi, D.P., Chang, S.J., Planavsky, N.J., 2021. Oxygen isotopic fingerprints on the phosphorus cycle within the deep subseafloor biosphere. Geochim. Cosmochim. Ac. 310, 169–186.
Zohar, I., Shaviv, A., Klass, T., Roberts, K., Paytan, A., 2010. Method for the analysis of oxygen isotopic composition of soil phosphate fractions. Environ. Sci. Technol. 44, 7583–7588.